Water Science & Technology

IWA PUBLISHING

Water Science & Technology Vol 88 No 6, 1428 doi: 10.2166/wst.2023.282

Catalytic polymerization of bisphenol A using a horseradish peroxidase immobilized microporous membrane reactor

Haitao Li[a,*,†], Linfeng Guo[a,†], Yingying Li[b,†], Min Chen[a], Chunlu Bai[c], Aolei Song[c], Linxiu Cheng[a], Xueli Chen[a] and Yonglin Chen[a]

[a] Jiangxi Provincial Key Laboratory of Low-Carbon Solid Waste Recycling, School of Geography and Environmental Engineering, Gannan Normal University, Ganzhou 341000, China
[b] Semiconductor Manufacturing North China (Beijing) Co., Ltd, Beijing, China
[c] Beijing Changzheng Mechanical Equipment Manufacture Co., Ltd, Beijing, China
*Corresponding author. E-mail: lihaitao103904@126.com
†Yingying Li, Linfeng Guo and Haitao Li were the first authors.

ABSTRACT

Bisphenol A (BPA) is one of the most widely used chemical products, which is discharged into rivers and oceans, posing great hazards to organisms such as reproductive toxicity, hormone imbalance and cardiopathy induction. With the expansion harm of BPA, people have paid more attention to the environmental effects. In this paper, the degradation of BPA from the synthetic wastewater using the immobilization of horseradish peroxidase membrane reactor (HPR) was investigated. The immobilized HRP microporous membrane was prepared by the porous calcium alginate method. In addition, the reuse of the immobilized HPR membrane and the measurement of membrane flux showed that the membrane has good activity and stability. Finally, the experimental parameters including reaction time, pH, the concentration of BPA and the dosage of H_2O_2 were optimized to remove the BPA, and about 78% degradation efficiency of BPA was achieved at the optimal condition as follows: H_2O_2 to BPA molar ratio of 1.50 with an initial BPA concentration of 0.1 mol/L, the HPR dosage of 3.84 u/mL, the initial solution pH of 7.0, a temperature of 20 °C and a contact time of 10 min.

Key words: Bisphenol A, enzymatic catalysis, horseradish peroxidase, microporous ultrafiltration membrane, water pollution remediation

HIGHLIGHTS

- Horseradish peroxidase (HRP) can be effectively immobilized on the membrane.
- The immobilized HRP can maintain high activity and be circulation utilization.
- The optimum conditions for the mole rate of H_2O_2/BPA dosage and the pH value are 1.5 and 7, respectively.

1. INTRODUCTION

Water is an essential foundation for the environment and life, which has been seriously polluted by organic contaminants in recent years (Chen *et al.* 2021; Al-Qadri *et al.* 2022). Many organic pollutants in the water bodies cause serious environmental problems to ecosystems and human health due to their persistent, high solubility, and high toxic and carcinogenic properties (Wang *et al.* 2015a, 2015b; Ribeiro *et al.* 2017; Wu *et al.* 2023). For example, the animals' long time exposure to the bisphenol A (BPA)-contained ($\geq$ ng/L) water bodies could causes disrupt endocrine, symptoms of sexual maturation and alter their reproductive function (Moussavi *et al.* 2018). BPA is a typical environmental endocrine disruptor, belonging to environmental hormones. As a widely used plasticizer, it is widely used in the synthesis and decomposition process of materials in the plastic industry and the electronic industry (Yu *et al.* 2022). In addition, BPA can coexist with pollutants such as microplastics, heavy metals, pesticides, antibiotics and polyaromatic hydrocarbons in wastewater, and cannot be completely degraded in water or soil for decades (Adu-Gyamfi *et al.* 2022). Therefore, these have spurred intensive efforts to develop novel sustainable technologies for the cleanliness of these organic contaminants.

As an efficient and green biocatalyst, enzymes are widely used in wastewater treatment because of their good specificity, high catalytic efficiency and mild reaction conditions (Fernández-Fernández *et al.* 2013). Horseradish peroxidase (HRP) is a typical oxidoreductase and is a versatile enzyme used in the pharmaceutical, chemical, biotechnology and environmental

industries (Chattopadhyay & Mazumdar 2000; Veitch 2004). When HRP is present, the oxidation of phenolic compound is catalyzed by the addition of H_2O_2 to form corresponding free radicals, and then, the free radicals spontaneously interact to quickly form insoluble polymers that can be easily removed from wastewater (Wang *et al.* 2015a, 2015b). However, in actual use, there are shortcomings such as poor operational stability, easy inactivation under extreme conditions, inability to reuse and recycle and high cost of use, which limit the further application of this technology (Sheldon 2007).

A large number of studies have found that the immobilization of enzymes by using carrier binding is one of the direct and effective methods to improve the catalytic efficiency of enzymes (Gasser *et al.* 2014; Mohamad *et al.* 2015). In order to obtain the ideal immobilization enzyme and improve the activity and stability of the immobilized enzyme, it is necessary to select an efficient immobilization method and a suitable immobilization vector (Kim *et al.* 2016; Patel *et al.* 2016, 2017). The membrane material is a good choice as a carrier for enzyme fixation, which combines the catalytic function of the enzyme with the separation function of the membrane (Vasconcelos *et al.* 2020). At the same time, with the selective transfer of membranes, reactants, reaction products and solvents can be separated, purified and enriched, so as to realize the two processes of enzyme-catalyzed reaction and separation in one system, which is an advantage that other carrier materials do not have (Girelli & Scuto 2021; Zhang *et al.* 2021). Escalona *et al.* (2014) used the enzyme-bound nanofiltration membrane to treat BPA to achieve a good removal effect, however, the production cost of nanofiltration membrane is relatively high, and the operating pressure of membrane filtration is large (Albergamo *et al.* 2019). In contrast, ultrafiltration is a low-pressure operation with the advantage of low cost and is more suitable for a wide range of applications in water treatment (Shi *et al.* 2014; Krahnstover *et al.* 2019; Ahmad *et al.* 2020).

In this study, HRP was fixed on the microporous ultrafiltration membrane by porous calcium alginate embedding (Aryal 2019; Meng *et al.* 2020), and the rich pore structure of the membrane provided an excellent matrix for the loading of HRP, and the small pore size of the membrane promoted the contact between BPA and the catalyst, which catalyzed the conversion of BPA into polymer precipitation and helped its removal. With this design, the ultrafiltration membrane can realize the immobilization and reuse of HRP, while removing the polymer precipitation during the filtration process to obtain purified water. Then, the influence of immobilization on the catalytic activity of HRP was explored. Finally, the optimal process parameters of HRP immobilized membranes for actual industrial wastewater treatment are investigated, including the amount of H_2O_2, the initial concentration of BPA, pH and reaction time. This work is expected to provide a novel approach for the further development of the catalysis membrane system.

2. MATERIALS AND METHODS

2.1. Materials and reagents

HRP (lyophilized powder, 250 u/mg) was purchased from Shanghai Guchen Biotechnology Co., Ltd. BPA and Sodium alginate were purchased from Shanghai Aladdin Biochemical Technology Co., Ltd. Sodium dihydrogen phosphate and disodium hydrogen phosphate were obtained by Sinopharm Chemical Reagent Co., Ltd. Hydrogen peroxide 3% (w/w), hydrochloric acid, sodium hydroxide and calcium chloride were supplied from Shanghai Macklin Biochemical Co., Ltd. All the chemical reagents except hydrogen peroxide in experiment were analytically pure grade.

An electronic balance (ME204/02) was used to weigh the reagent. The concentration of BPA was analyzed by a UV–Vis spectrophotometer (UV, BlueStar A). A pipette gun (200 and 5,000 μL) was used to pick up the liquid. The HRP was loaded on an ultrafiltration filter (φ100 mm, membrane pore size 0.22 μm, PES). The ultrafiltration filter membrane was purchased from Tianjin Navigator Lab Instrument Institute.

The surface morphology and structure were characterized using a Supra55 Scanning Electron Microscope (SEM), and nitrogen gas purging was performed on the membrane section in advance. The acceleration voltage of the instrument was 20.00 kV, the working distance was 8.2 mm, the magnification was 7,940 times and the detector was SE2.

The configuration method of synthetic wastewater is as follows: a certain amount of BPA powder is weighed and dissolved in a beaker, and then, the volume is fixed with a volumetric flask to obtain a simulated synthetic wastewater containing a BPA concentration of 0.2 mmol/L.

The determination of BPA was as follows: it was determined at the characteristic absorption wavelength of 510 nm by a UV–Vis Spectrophotometer ($R^2 = 0.9997$). According to the following formula to calculate the removal rate of BPA: $\eta = (A_0 - A_t)/A_0 \times 100\%$, where η is the removal rate of BPA, A_0 is the initial absorbance of BPA and A_t is the absorbance of BPA after the reaction.

2.2. Immobilization of HRP

The HPR was immobilized on the microporous membrane through the porous calcium alginate method. The specific process of the immobilization method was as follows: 0.25 g of sodium alginate was dissolved into 100 mL of distilled water; meanwhile, 120 mg of HRP was dissolved in 10 mL phosphate buffer solution of pH 7.0, and after that 1.5 mL of sodium alginate solution and 1.5 mL of HRP solution were thoroughly mixed. Then, the whole mixture was evenly coated on the microporous membrane and allowed to stand for 10 min. Next, the microporous membrane was placed in 0.1 mol/L calcium chloride solution and allowed to stand for 20 min. Finally, the embedded membrane was placed indoors for 2.5 h, the prepared enzymatic membranes were stored in phosphate buffer solution for use (Figure 1).

2.3. Experimental procedure

The 100 mL of BPA was pumped into the reactor through the peristaltic pump. A portion of the solution, which is backwater, flowed through the surface of the microporous filter and reacted with the HPR on the surface of the membrane. The other part of the solution, which is the final water, passed through the microporous filter under pressure and reacted with HPR in the membrane pore. Finally, these two parts of the liquid were returned to the beaker. The flowchart of the reaction mechanism is shown in Figures 1 and 2. All experiments were conducted in two or more parallel experiments. The removal of BPA (%) was calculated according to the following formula:

$$\text{The removal of BPA} = \frac{C_0 - C_t}{C_0} \times 100\%$$

In the formula, C_0 (mmol/L) is the initial concentration of BPA in wastewater and C_t (mmol/L) is the concentration of BPA in wastewater after a certain period of time.

The main factors of this study are the reuse effect of HRP; reaction time; the mole ratio of H_2O_2/BPA, including 1:1, 1.5:1, 2:1 and 2.5:1; the initial concentrations of BPA, including 0.025, 0.05, 0.1, 0.15 and 0.20 mmol/L and the initial pH of the solution includes 4, 6, 7, 8 and 10.

3. RESULTS AND DISCUSSION

3.1. Characterization of the HRP membrane

The surface morphology and structure of the immobilized HRP membrane were characterized by SEM images. Figure 3(a)–3(c) shows the microporous membrane, the unreacted of HRP membrane and the reaction of HRP membrane with BPA. There

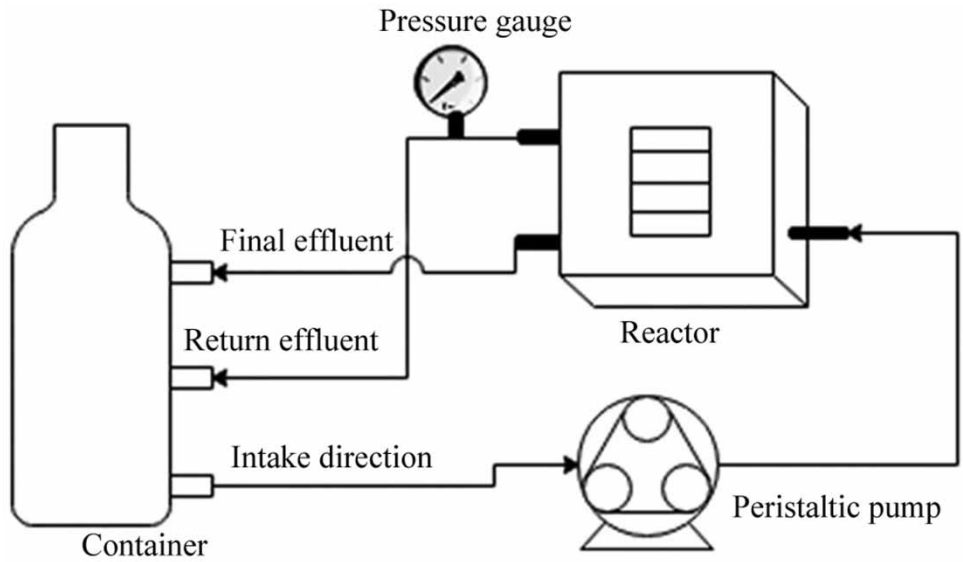

Figure 1 | Flowchart of the enzyme catalysis reaction.

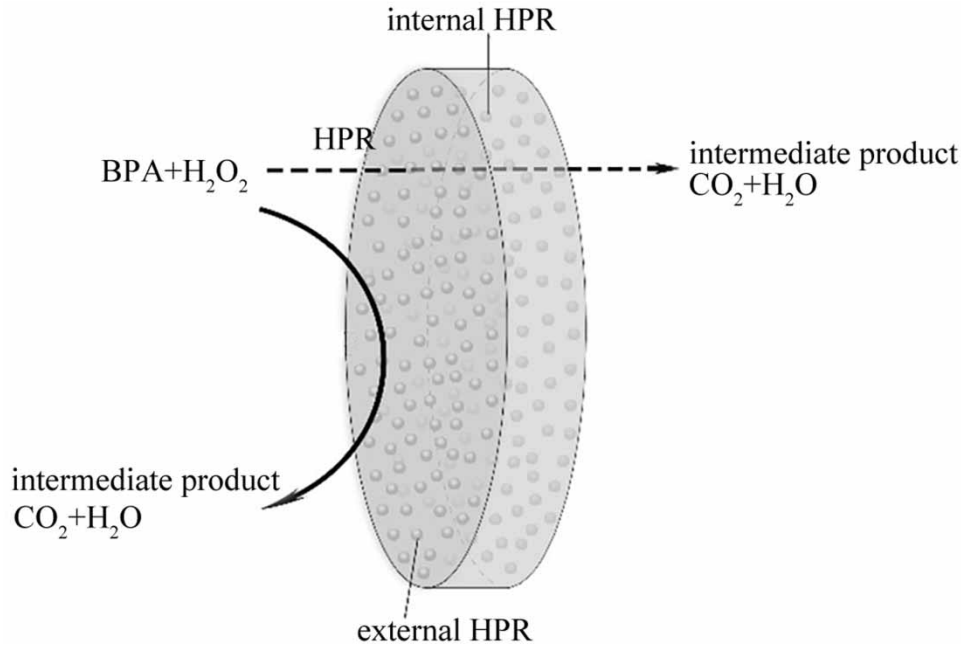

Figure 2 | Schematic diagram of the reaction mechanism of the HPR immobilized membrane.

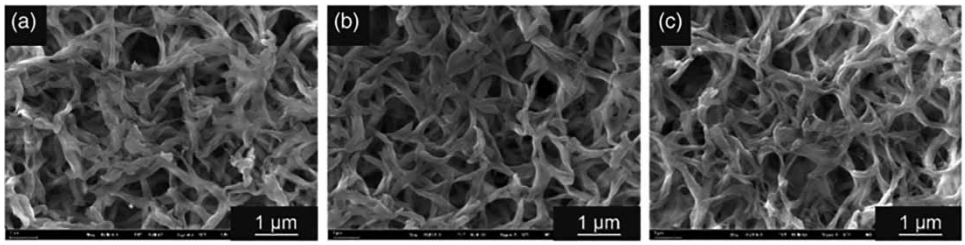

Figure 3 | SEM image of microporous membrane (a), the unreacted of HRP membrane (b) and the reaction of HRP membrane (c).

was an uneven distribution aperture on the surface of microporous membrane; a small amount of filamentous reticular substance can be observed when HPR was immobilized on the microporous membrane. It was shown that HPR was attached to the three-dimensional void of the microporous membrane. After the reaction, the membrane still retained more three-dimensional pores, which indicated that most of the membrane pores were not blocked.

3.2. Investigation on the activity of immobilized enzyme

In the immobilized catalytic membrane system, a key problem that cannot be ignored is the reusability of the catalytic membrane. The catalyst on the membrane surface is easily inactivated during long-term filtration. Unfortunately, conventional catalyst regeneration methods, such as high-temperature calcination or washing with organic solvents, are not suitable for immobilized catalytic membrane systems (Li *et al.* 2019). Therefore, to investigate the stability of the immobilized HRP membrane, the membrane was recovered and reused after each experiment (Sri Kaja *et al.* 2018). The result in Figure 4 showed that the HRP membranes have considerable reusability for the degradation of BPA and the degradation rate decreased from 73.3 to 56.8% after being used for four recycles. The activity of immobilized HRP decreased with the increase of the times of reuses. The result showed that the immobilized HRP still maintained high activity after being used for four times. Therefore, the HPR membrane can be circulation utilization. Immobilized enzymes are prone to deformation and inactivation in harsh environments, and their stability is greatly affected in practical applications. Therefore, studies on the activity and recyclability of the immobilized enzyme are very necessary.

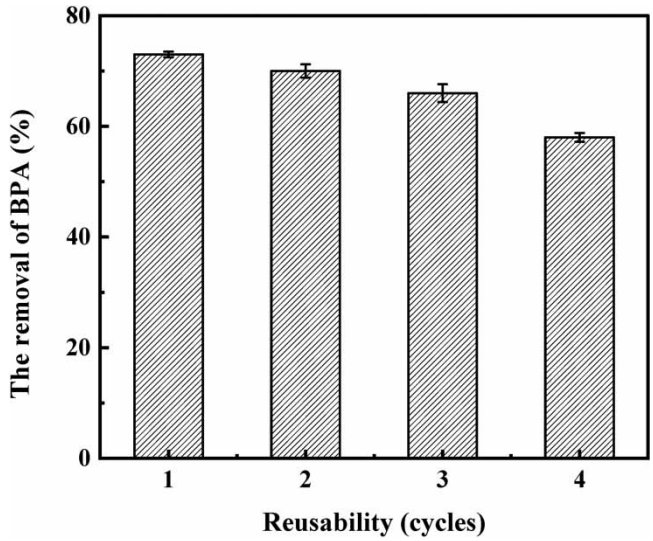

Figure 4 | Stability of the catalytic activity of HRP membrane ($C_{BPA} = 0.1$ mmol/L, $n_{H_2O_2}$:$n_{BPA} = 1.5$:1, the dosage of HRP = 3.84 u/mL, pH = 7, $T = 20$ °C).

Membrane flux is related to the ability of a membrane to remove contaminants. Ultrafiltration membranes can effectively remove insoluble polymers and water from wastewater. However, the permeation flux is reduced due to membrane contamination during filtration. The polymer deposited on the surface of the ultrafiltration membrane or the low polymer in the pores will lead to a decrease in the permeation flux of the membrane under the same pressure (Onishi & Kamimori 2013). Table 1 shows that the water flux of the membranes was used four times at 0.065 and 0.08 MPa. It could be seen that the higher the pressure, the greater the value of the water flux. And with the increase in the usage count of the HPR membrane, the value of water flux decreased slightly. The performance of the ultrafiltration membrane can be maintained by cleaning the membrane with air washing, reverse washing, chemical cleaning, etc., but it will eventually shorten the service life of the membrane (Akther *et al.* 2020).

3.3. Effect of reaction time on the degradation of BPA

The degradation of BPA was conducted as shown in Figure 5. With the increase in reaction time, the removal rate of BPA rapidly increased in the initial 5 min and then slowly in 5–60 min. The removal rates of BPA were 71.5% in 5 min and 76.8% in 60 min, respectively. This result showed that the degradation of BPA rapidly increased with the increase in reaction time, and it tended to be steady. When the reaction reached equilibrium, no significant changes in removal rates were observed over time. It indicated that further increased reaction time (>5 min) had little effect on the BPA degradation. Therefore, the reaction time of the follow-up experiment was 10 min, and the optimum reaction time was 10 min.

3.4. Effect of the dosage of H_2O_2 on the degradation of BPA

In the absence of H_2O_2, it is difficult to perform biocatalytic reactions by immobilized HPR alone. Studies have shown that the removal efficiency of phenolic compounds can be improved by choosing the appropriate H_2O_2 concentration (Wu *et al.*

Table 1 | The pure water flux of the HPR membrane under different pressures

	Membrane flux (L/(m² h))	
Test time	**Test 1 (Pressure: 0.08 MPa)**	**Test 2 (Pressure: 0.065 MPa)**
1st	301.3	222.0
2nd	286.8	214.8
3rd	288.0	216.0
4th	260.4	205.2

Membrane reactor system ($C_{BPA} = 0.1$ mmol/L, $n_{H_2O_2}$:$n_{BPA} = 1.5$:1, the dosage of HRP = 3.84 u/mL, pH = 7, $T = 20$ °C).

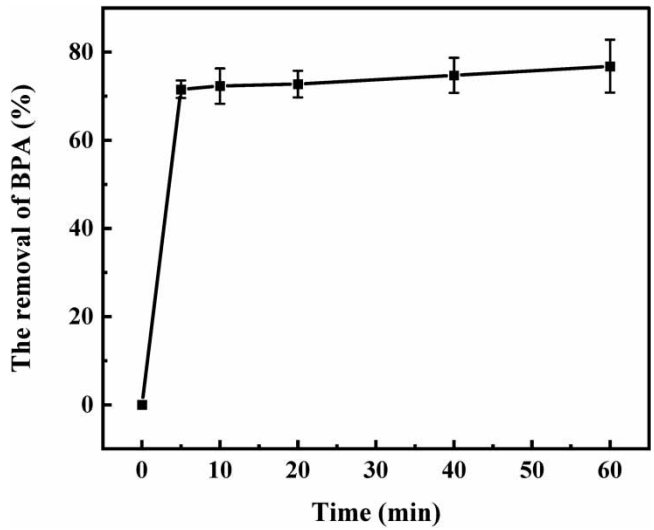

Figure 5 | Effect of the reaction time on the removal of BPA in immobilized enzymatic (C_{BPA} = 0.1 mmol/L, $n_{H_2O_2}$:n_{BPA} = 1.5:1, the dosage of HRP = 3.84 u/mL, pH = 7, T = 20 °C).

2022). As shown in Figure 6, the influences of H_2O_2 on the degradation of BPA were investigated. The removal rate of BPA was only 71.9% when the mole ratio of H_2O_2/BPA was 1:1. When the mole ratio of H_2O_2/BPA increased to 1.5, the removal rate of BPA reached 78.6%. When the mole ratio of H_2O_2/BPA was higher than 1.5, the degradation efficiency of BPA had a tendency to decrease. It was obviously observed that the excessive addition of H_2O_2 dosage could inhibit the degradation of BPA. That may be because the overdosage of H_2O_2 could result in the production of intermediate products that might inhibit the oxidation capacity of HRP (Wang *et al.* 2015a, 2015b). In addition, H_2O_2 could act as scavengers of active radicals through reduction reactions (Ai *et al.* 2017). Therefore, the optimum n(H_2O_2):n(BPA) was 1.5.

In general, the amount of H_2O_2 added directly affects the efficiency of HRP in removing BPA; too low a concentration will not achieve the desired removal effect, and too high a concentration will inhibit the degradation of BPA, thus affecting the removal efficiency. Therefore, it is necessary to explore the effect of hydrogen peroxide concentration on BPA. At the same

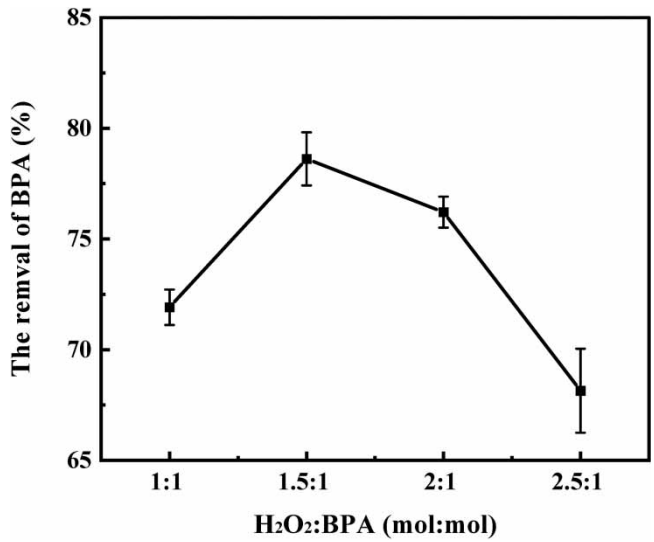

Figure 6 | Effect of H_2O_2 dosage on the degradation of BPA in the immobilized enzymatic membrane reactor system. (C_{BPA} = 0.1 mmol/L, reaction time of 10 min, the dosage of HRP = 3.84 u/mL, pH = 7, T = 20 °C).

time, the cost of H_2O_2 is high in practical applications, so it is of great economic significance to choose the appropriate concentration of H_2O_2.

3.5. Effect of the initial concentration of BPA

The degradation of phenolic compounds by HRP was closely related to the initial concentration of phenolic compounds (Moussavi *et al.* 2018). In the actual treatment of wastewater, the concentration of BPA in wastewater is variable, and different concentrations have different removal effects. The applicability of the immobilized HRP membrane system to changes in water quality was investigated by measuring the removal efficiency of BPA at different concentrations of BPA (Zhao *et al.* 2021).

The effect of the initial concentration of BPA on the removal rate is shown in Figure 7. When the initial concentration of BPA was 0.025, 0.05, 0.1 and 0.2 mmol/L, the removal rate of BPA in the immobilized HPR membrane process was 92.2, 75.4, 68.3 and 61.6%, respectively. It was observed that the degradation rate of BPA gradually decreased with the increase of the initial concentration of BPA. Obviously, the insufficiency of available HPR led to the decrease of degradation efficiency of BPA with the increase of BPA concentration.

3.6. Effect of solution pH on the degradation of BPA

For free/immobilized enzyme, pH was one of the most important influence factors on enzyme activity. In general, all enzymes have an optimum pH at which their activity is greatest, but not necessarily the same as their normal intracellular environment (Hu *et al.* 2018). It was necessary to investigate the degradation of BPA by the immobilized HRP membrane system in different solution pH values. The effect of pH on the degradation of BPA was investigated in the pH range of 4.0–10.0 and the obtained result is shown in Figure 8. When the initial pH increased from 4.0 to 7.0, the removal of BPA obviously increased from 69.2 to 77.6%. The removal rate of BPA was 72.7 and 68.9% at pH 8.0 and 10.0. As can be seen, the optimum pH was 7 and the removal of BPA was slightly inhibited in acid and alkaline conditions.

The results showed that immobilized HPR was able to oxidize BPA over the entire pH range studied, indicating that HRP was active over a wide pH range. The results are consistent with those reported previously in the literature, and the reason for the lower efficiency of BPA removal may be the increased instability of HRP under non-optimal pH conditions, leading to loss of enzyme activity (Zhang *et al.* 2022). At the same time, it may also be that the interaction between BPA and HPR is reduced (Yamada *et al.* 2010).

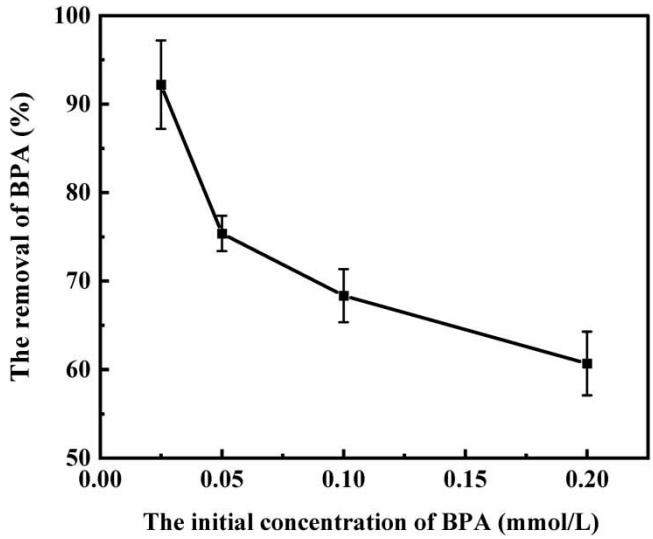

Figure 7 | Effect of the initial concentration of BPA on the degradation of BPA for the immobilized enzymatic membrane reactor system (reaction time of 10 min, $n_{H_2O_2}$:n_{BPA} = 1.5:1, pH = 7, T = 20 °C).

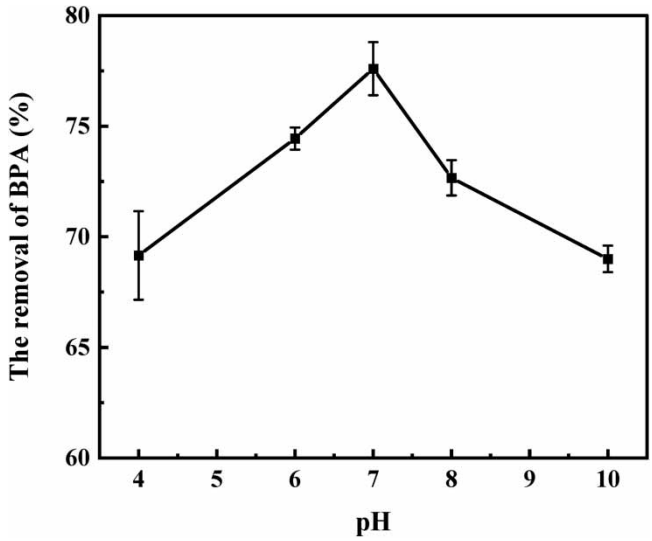

Figure 8 | Effect of pH on the degradation of phenol in the immobilized enzymatic membrane reactor system ($C_{BPA} = 0.1$ mmol/L, reaction time of 10 min, the dosage of HRP = 3.84 u/mL, $n_{H_2O_2}$:$n_{BPA} = 1.5$:1).

4. CONCLUSION

In this paper, the application of the immobilized HPR microporous membrane reactor system for the degradation of BPA from aqueous solution was investigated. When HRP is present, BPA is catalyzed by the addition of H_2O_2 to form corresponding free radicals, and then, the free radicals spontaneously interact to quickly form insoluble polymers that can be easily removed from wastewater. The results showed that this strain had a high degradation efficiency for BPA. In addition, the reusability experiment showed that the immobilized HPR membrane can be used up to four times without serious deficiency in its activity and water flux of the membrane. The removal rate of BPA by the immobilized HPR membrane tended to be balanced after 10 min reaction. The removal rate of BPA increased initially and then decreased with the increase of H_2O_2 dosage and the solution pH value. The optimum conditions for the mole rate of H_2O_2/BPA dosage and the pH value are 1.5 and 7, respectively. In summary, under the conditions of HPR dosage of 3.84 u/mL, initial solution pH of 7.0, temperature of 20 °C, contact time of 10 min and molar ratio of H_2O_2 to BPA of 1.50, the optimal degradation efficiency of BPA was 78%. In conclusion, the immobilized HPR membrane reactor system was a considerable potential method for the efficient treatment of BPA effluents.

ACKNOWLEDGEMENTS

This work was supported by the National Natural Science Foundation of China (52260022); Jiangxi Provincial Natural Science Foundation (20224BAB213031); Science and Technology Research Project of Jiangxi Provincial Department of Education (GJJ201416) and the Open Research Fund Program of Jiangxi Provincial Key Laboratory of Low-Carbon Solid Waste Recycling (20212BCD42015).

DATA AVAILABILITY STATEMENT

All relevant data are included in the paper or its Supplementary Information.

CONFLICT OF INTEREST

The authors declare there is no conflict.

REFERENCES

Adu-Gyamfi, E. A., Rosenfeld, C. S. & Tuteja, G. 2022 The impact of bisphenol A on the placenta. *Biology of Reproduction* **106** (5), 826–834. doi:10.1093/biolre/ioac001.

Ahmad, T., Guria, C. & Mandal, A. 2020 A review of oily wastewater treatment using ultrafiltration membrane: a parametric study to enhance the membrane performance. *Journal of Water Process Engineering* **36**, 101289. doi:10.1016/j.jwpe.2020.101289.

Ai, J., Zhang, W., Liao, G., Xia, H. & Wang, D. 2017 $NH_2Fe_3O_4$@SiO_2 supported peroxidase catalyzed H_2O_2 for degradation of endocrine disrupter from aqueous solution: roles of active radicals and NOMs. *Chemosphere* **186**, 733–742. doi:10.1016/j.chemosphere.2017.08.039.

Akther, N., Ali, S. M., Phuntsho, S. & Shon, H. 2020 Surface modification of thin-film composite forward osmosis membranes with polyvinyl alcohol-graphene oxide composite hydrogels for antifouling properties. *Desalination* **491**, 11. doi:10.1016/j.desal.2020.114591.

Albergamo, V., Blankert, B., Cornelissen, E. R., Hofs, B., Knibbe, W., van der Meer, W. & de Voogt, P. 2019 Removal of polar organic micropollutants by pilot-scale reverse osmosis drinking water treatment. *Water Research* **148**, 535–545. doi:10.1016/j.watres.2018.09.029.

Al-Qadri, A. A. Q., Drmosh, Q. A. & Onaizi, S. A. 2022 Enhancement of bisphenol a removal from wastewater via the covalent functionalization of graphene oxide with short amine molecules. *Case Studies in Chemical and Environmental Engineering* **6**, 100233. doi:10.1016/j.cscee.2022.100233.

Aryal, M. 2019 Calcium alginate entrapped *Eupatorium adenophorum* Sprengel stems powder for chromium(VI) biosorption in aqueous mediums. *PLoS One* **14** (8), e213477. doi:10.1371/journal.pone.0213477.

Chattopadhyay, K. & Mazumdar, S. 2000 Structural and conformational stability of horseradish peroxidase: effect of temperature and pH. *Biochemistry-US* **39** (1), 263–270. doi:10.1021/bi990729o.

Chen, X., Li, F., Zhang, M., Liu, B., Chen, H. & Wang, H. 2021 Highly dispersed and stabilized Co_3O_4/C anchored on porous biochar for bisphenol A degradation by sulfate radical advanced oxidation process. *Science of the Total Environment* **777**, 145794. doi:10.1016/j.scitotenv.2021.145794.

Escalona, I., de Grooth, J., Font, J. & Nijmeijer, K. 2014 Removal of BPA by enzyme polymerization using NF membranes. *Journal of Membrane Science* **468**, 192–201. doi:10.1016/j.memsci.2014.06.011.

Fernández-Fernández, M., Sanromán, M. Á. & Moldes, D. 2013 Recent developments and applications of immobilized laccase. *Biotechnology Advances* **31** (8), 1808–1825. doi:10.1016/j.biotechadv.2012.02.013.

Gasser, C. A., Ammann, E. M., Shahgaldian, P. & Corvini, P. F. X. 2014 Laccases to take on the challenge of emerging organic contaminants in wastewater. *Applied Microbiology and Biotechnology* **98** (24), 9931–9952. doi:10.1007/s00253-014-6177-6.

Girelli, A. M. & Scuto, F. R. 2021 Eggshell membrane as feedstock in enzyme immobilization. *Journal of Biotechnology* **325**, 241–249. doi:10.1016/j.jbiotec.2020.10.016.

Hu, L., Zhang, G., Liu, M., Wang, Q. & Wang, P. 2018 Enhanced degradation of bisphenol A (BPA) by peroxymonosulfate with Co_3O_4-Bi_2O_3 catalyst activation: effects of pH, inorganic anions, and water matrix. *Chemical Engineering Journal (Lausanne, Switzerland: 1996)* **338**, 300–310. doi:10.1016/j.cej.2018.01.016.

Kim, T., Patel, S. K. S., Selvaraj, C., Jung, W., Pan, C., Kang, Y. C. & Lee, J. 2016 A highly efficient sorbitol dehydrogenase from *Gluconobacter oxydans* g624 and improvement of its stability through immobilization. *Scientific Reports* **6** (1). doi:10.1038/srep33438.

Krahnstover, T., Hochstrat, R. & Wintgens, T. 2019 Comparison of methods to assess the integrity and separation efficiency of ultrafiltration membranes in wastewater reclamation processes. *Journal of Water Process Engineering* **30**, 8. doi:10.1016/j.jwpe.2018.06.008.

Li, N., Chen, G., Zhao, J., Yan, B., Cheng, Z., Meng, L. & Chen, V. 2019 Self-cleaning PDA/ZIF-67@PP membrane for dye wastewater remediation with peroxymonosulfate and visible light activation. *Journal of Membrane Science* **591**, 9. doi:10.1016/j.memsci.2019.117341.

Meng, F., Li, M., Wang, H., Xin, L., Wu, X. & Liu, X. 2020 Encapsulating microscale zero valent iron-activated carbon into porous calcium alginate for the improvement on the nitrate removal rate and Fe^0 utilization factor. *Microporous and Mesoporous Materials* **307**, 110522. doi:10.1016/j.micromeso.2020.110522.

Mohamad, N. R., Marzuki, N. H. C., Buang, N. A., Huyop, F. & Wahab, R. A. 2015 An overview of technologies for immobilization of enzymes and surface analysis techniques for immobilized enzymes. *Biotechnology & Biotechnological Equipment* **29** (2), 205–220. doi:10.1080/13102818.2015.1008192.

Moussavi, G., Pourakbar, M., Shekoohiyan, S. & Satari, M. 2018 The photochemical decomposition and detoxification of bisphenol A in the VUV/H_2O_2 process: degradation, mineralization, and cytotoxicity assessment. *Chemical Engineering Journal* **331**, 755–764. doi:10.1016/j.cej.2017.09.009.

Onishi, M. & Kamimori, H. 2013 High-throughput and sensitive assay for amphotericin B interaction with lipid membrane on the model membrane systems by surface plasmon resonance. *Biological and Pharmaceutical Bulletin* **36** (4), 6.

Patel, S. K., Choi, S. H., Kang, Y. C. & Lee, J. K. 2016 Large-scale aerosol-assisted synthesis of biofriendly Fe_2O_3 yolk-shell particles: a promising support for enzyme immobilization. *Nanoscale* **8** (12), 6728–6738. doi:10.1039/c6nr00346j.

Patel, S. K. S., Choi, S. H., Kang, Y. C. & Lee, J. 2017 Eco-friendly composite of Fe_3O_4-reduced graphene oxide particles for efficient enzyme immobilization. *ACS Applied Materials & Interfaces* **9** (3), 2213–2222. doi:10.1021/acsami.6b05165.

Ribeiro, E., Ladeira, C. & Viegas, S. 2017 Occupational exposure to bisphenol A (BPA): a reality that still needs to be unveiled. *Toxics* **5** (3), 22. doi:10.3390/toxics5030022.

Sheldon, R. A. 2007 Enzyme immobilization: the quest for optimum performance. *Advanced Synthesis & Catalysis* **349** (8–9), 1289–1307. doi:10.1002/adsc.200700082.

Shi, X., Tal, G., Hankins, N. P. & Gitis, V. 2014 Fouling and cleaning of ultrafiltration membranes: a review. *Journal of Water Process Engineering* **1**, 18. doi:10.1016/j.jwpe.2014.04.003.

Sri Kaja, B., Lumor, S., Besong, S., Taylor, B. & Ozbay, G. 2018 Investigating enzyme activity of immobilized *Candida rugosa* lipase. *Journal of Food Quality* **2018**, 1–9. doi:10.1155/2018/1618085.

Vasconcelos, N. F., Andrade, F. K., Vieira, L. D. A. P., Vieira, R. S., Vaz, J. M., Chevallier, P., Mantovani, D., Borges, M. D. F. & Rosa, M. D. F. 2020 Oxidized bacterial cellulose membrane as support for enzyme immobilization: properties and morphological features. *Cellulose (London)* **27** (6), 3055–3083. doi:10.1007/s10570-020-02966-5.

Veitch, N. C. 2004 Horseradish peroxidase: a modern view of a classic enzyme. *Phytochemistry* **65** (3), 249–259. doi:10.1016/j.phytochem.2003.10.022.

Wang, S., Fang, H., Wen, Y., Cai, M., Liu, W., He, S. & Xu, X. 2015a Applications of HRP-immobilized catalytic beads to the removal of 2,4-dichlorophenol from wastewater. *RSC Advances* **5** (71), 7. doi:10.1039/c5ra08688d.

Wang, S., Wang, L., Hua, W., Zhou, M., Wang, Q., Zhou, Q. & Huang, X. 2015b Effects of bisphenol A, an environmental endocrine disruptor, on the endogenous hormones of plants. *Environmental Science and Pollution Research* **22** (22), 17653–17662. doi:10.1007/s11356-015-4972-y.

Wu, J., Ma, X., Li, C., Zhou, X., Han, J., Wang, L., Dong, H. & Wang, Y. 2022 A novel photon-enzyme cascade catalysis system based on hybrid HRP-CN/$Cu_3(PO_4)_2$ nanoflowers for degradation of BPA in water. *Chemical Engineering Journal* **427**, 10. doi:10.1016/j.cej.2021.131808.

Wu, J., Ma, X., He, T., Han, J., Zhu, Y., Li, C. & Wang, Y. 2023 A photo-enzyme coupling catalysis system with high enzyme loading for the efficient degradation of BPA in water. *Separation and Purification Technology* **313**, 123392. https://doi.org/10.1016/j.seppur.2023.123392.

Yamada, K., Ikeda, N., Takano, Y., Kashiwada, A., Matsuda, K. & Hirata, M. 2010 Determination of optimum process parameters for peroxidase-catalysed treatment of bisphenol A and application to the removal of bisphenol derivatives. *Environmental Technology* **31** (3), 243–256. doi:10.1080/09593330903453228.

Yu, Y., Xin, X., Ma, F., Li, X., Wang, Y., Zhu, Q., Chen, H., Li, H. & Ge, R. 2022 Bisphenol AF blocks Leydig cell regeneration from stem cells in male rats. *Environmental Pollution* **298**, 118825. doi:10.1016/j.envpol.2022.118825.

Zhang, H., Gao, S. & Sheng, G. 2021 Immobiling enzyme-like ligand in the ultrafiltration membrane to remove the micropollutant for the ultrafast water purification. *Journal of Membrane Science* **636**, 119566. doi:10.1016/j.memsci.2021.119566.

Zhang, R., Yu, J., Zhang, T., Zhao, C., Han, Q., Li, Y., Liu, Y., Zeng, K., Cai, L., Yang, Z. & Ma, Y. 2022 A novel snowflake dual Z-scheme Cu_2S/RGO/Bi_2WO_6 photocatalyst for the degradation of bisphenol A under visible light and its effect on crop growth. *Colloids and Surfaces A: Physicochemical and Engineering Aspects* **641**, 128526. doi:10.1016/j.colsurfa.2022.128526.

Zhao, C., Zhang, G. & Jiang, J. 2021 Enhanced phytoremediation of bisphenol A in polluted lake water by seedlings of *Ceratophyllum demersum* and *Myriophyllum spicatum* from in vitro culture. *International Journal of Environmental Research and Public Health* **18** (2), 810. doi:10.3390/ijerph18020810.

First received 18 April 2023; accepted in revised form 8 August 2023. Available online 1 September 2023